Minerals Engineering 213 (2024) 108754

Contents lists available at ScienceDirect

Minerals Engineering

journal homepage: www.elsevier.com/locate/mineng

CatBoost-SHAP for modeling industrial operational flotation variables – A “conscious lab” approach

Saeed Chehreh Chelgani [a,b,*], Arman Homafar [c], Hamid Nasiri [d], Mojtaba Rezaei laksar [e]

[a] Minerals and Metallurgical Engineering, Dept. of Civil, Environmental and Natural Resources Engineering, Luleå University of Technology, SE-971 87 Luleå, Sweden
[b] Wallenberg Initiative Materials Science for Sustainability, Department of Civil, Environmental and Natural Resources Engineering, Swedish School of Mines, Luleå University of Technology, Luleå, Sweden
[c] Electrical and Computer Engineering Department, Semnan University, Semnan, Iran
[d] Department of Computer Engineering, Amirkabir University of Technology (Tehran Polytechnic), Tehran, Iran
[e] Delijan Copper Flotation Company, Delijan, Iran

ARTICLE INFO

Keywords:
Random forest
Support vector regression
Extreme gradient boosting
Flotation circuit
Sodium ethyl xanthate
Potassium amyl xanthate

ABSTRACT

Flotation separation is the most important upgrading critical raw material technique. Measuring interactions within flotation variables and modeling their metallurgical responses (grade and recovery) is quite challenging on the industrial scale. These challenges are because flotation separation includes several sub-micron processes, and their monitoring won’t be possible for the processing plants. Since many flotation plants are still manually operating and maintaining, understanding interactions within operational variables and their effect on the metallurgical responses would be crucial. As a unique approach, this study used the “Conscious Lab” concept for modeling flotation responses of an industrial copper upgrading plant when Potassium Amyl Xanthate substituted the secondary collector (Sodium Ethyl Xanthate) in the process. The main aim is to understand and compare interactions before and after the collector substitution. For the first time, the conscious lab was constructed based on the most advanced explainable artificial intelligence model, Shapley Additive Explanations, and Catboost. Catboost- Shapley Additive Explanations could accurately model flotation responses (less than 2% error between actual and predicted values) and illustrate variations of complex interactions through the substitution. Through a comparative study, Catboost could generate more precise outcomes than other known artificial intelligence models (Random Forest, Support Vector Regression, Extreme Gradient Boosting, and Convolutional Neural Network). In general, substituting Sodium Ethyl Xanthate by Potassium Amyl Xanthate reduced process predictability, although Potassium Amyl Xanthate could slightly increase the copper recovery.

1. Introduction

Digitalizing industrial processes would enhance efficiency, consistency, and product quality. Integrating recorded information from different monitored units and operational variables into a digitalized form can potentially be used to predict the process responses (Sasikumar et al., 2022; Xu et al., 2021). Froth flotation, as the most frequent separation method through mineral processing, has a substantial role in producing and upgrading critical raw materials. Flotation separates minerals (or materials in terms of recycling) based on several micron and submicron processes, making it a complex system depending on several probabilities (Ghaffari et al., 2012; Chelgani et al., 2010; Nazari et al., 2019; Je et al., 2022). Thus, digitalizing and transferring flotation operational information of an ore dressing plant into a model would assist in optimizing its metallurgical responses (recovery and grade), understanding potential interactions, training personnel, and reducing cost and upscaling of laboratory experiments.

Several investigations have been conducted to model mineral flotation separation based on various variables that potentially would be effective on the process responses. Artificial neural network (*ANN*) models are the most applied artificial intelligence (*AI*) methods, which are mainly built based on laboratory datasets (Jorjani et al., 2008; Abdulhussein and Alwared, 2019; N.-N. Zhang et al., 2017; Al-Thyabat, 2009) and rarely on the industrial scale by image processing for froth (Table 1) (Fu and Aldrich, 2018). The essential issue with *ANN* models is that they are black boxes and do not provide insight into operational

* Corresponding author at: Minerals and Metallurgical Engineering, Dept. of Civil, Environmental and Natural Resources Engineering, Luleå University of Technology, SE-971 87 Luleå, Sweden.
E-mail address: saeed.chelgani@ltu.se (S. Chehreh Chelgani).

https://doi.org/10.1016/j.mineng.2024.108754
Received 14 February 2024; Received in revised form 4 May 2024; Accepted 22 May 2024

Table 1
AI models and their input variables for the industrial modeling of flotation responses.

Model	Input Variables	Output	Ref.
Convolutional Neural Network (CNN)	Froth images	Recovery	(Zarie,Jahedsaravani, and Massinaei, 2020)
Recurrent Neural Network	Column level Airflow Pulp density Pulp pH Pulp flow Amina flow Starch flow Silica feed Iron feed	Recovery	(Pu et al., 2020)
CNN	Froth images	Ash content	(Z. Wen et al., 2021b)
Fuzzy Neural Network	Froth images	Concentrate-grade	(Ai et al., 2019)
CNN	Froth images	Concentrate-grade	(Fu and Aldrich, 2019)

Table 2
CL applications in various fields.

Model	Output	R^2	Ref.
Boosted Neural Network (BNN)	Power draw of an HPGR	0.95	(Tohry et al., 2021)
Boosted Neural Network (BNN)	Pressure before and after the industrial cement raw ball mill fan	0.77	(Fatahi et al., 2021)
Extreme Gradient Boosting (XGBoost)	Particle sizes produced by a HpGR	0.83	(Chehreh Chelgani et al., 2021b)
Extreme Gradient Boosting (XGBoost)	Metallurgical responses of a coal column flotation	0.96	(Chehreh Chelgani et al., 2021a)
Boosted Neural Network (BNN)	Metallurgical responses of coal Tri-Flo separators	0.98	(Alidokht et al., 2021)
Extreme Gradient Boosting (XGBoost)	Output temperature and motor power of a cement vertical roller mill	0.99	(Fatahi et al., 2022)
CatBoost	Particle size of overflow and recovered particles of an industrial hydrocyclone	0.93	(Chehreh Chelgani et al., 2023)
Extreme Gradient Boosting (XGBoost)	Induced draft fan current and kiln feed rate of cement rotary kiln	0.96	(Fatahi et al., 2023)

Table 3
The statistical description of operating variables for the Delijan copper flotation circuit.

Variables	Min	Max	Mean	STD
+149 μm (t/h)	2.70	22.44	10.52	2.86
+74 μm (t/h)	0.66	18.66	12.65	1.79
−74 μm (t/h)	62.44	94.42	76.83	3.95
MIBC (g/t)	37.89	235.46	101.63	30.74
SEX (g/t)	5.20	21.49	7.58	2.19
PAX (g/t)	0.00	8.94	5.60	0.85
SS (g/t)	0.00	134.32	34.58	12.92
SIPX (g/t)	10.53	34.92	16.78	1.89
Lime (kg/min)	200.00	1200.00	1038.09	119.63
Ball (kg)	0.00	2000.00	126.50	298.73
Cu recovery (%)Cu grade (%)	74.61 15.25	97.49 28.67	91.38 21.13	3.70 2.37

variable relationships (Bai et al., 2023; Jorjani et al., 2008; Kellner et al., 2022; Huang et al., 2022). Since several flotation plants (especially small plants) are yet operated manually, it would be necessary for operators to understand the interactions within operational parameters and their potential effect on the process metallurgical responses (Ai et al., 2019). The conscious lab (*CL*) concept can fill this gap, essentially where only conventional operating variables are available. As a most recent concept developed by Chehreh Chelgani team (Tohry et al., 2021), *CL* is a structure that translates complex industrial datasets into human-basis information by using explainable artificial intelligence (*XAI*) models (Table 2) (Fatahi et al., 2023; Fatahi et al., 2022; Chelgani et al., 2021a; Fatahi et al., 2021; Tohry et al., 2021). *XAIs* assess single and multivariable relationships (linearly-nonlinearly) and illustrate interactions among all variables in a database (Nasiri et al., 2021; van der Velden et al., 2022; Saeed Chehreh Chelgani, 2021). Such a translation illustration can enhance plant efficiency and productivity, decrease operational and laboratory costs, and promote operator understanding and faster decision-making (Homafar et al., 2022; C. A. Zhang et al., 2022).

CL has recently been used in modeling metallurgical responses of an industrial coal column flotation. It was reported that *CL* structure, SHapley Additive exPlanations (SHAP), and extreme gradient boosting (XGB) could accurately model the concentrate yield and separation efficiency of the plant based on monitored operational variables (feed solid percentage, frother dosage, collector dosage, airflow rate, washing water, froth level and feed specific gravity) (Chelgani et al., 2021a). However, *CL* was not used to monitor flotation reagent interactions on the industrial scale. Moreover, it was recently documented that CatBoost (CB), as the latest machine learning generation for prediction, is extraordinarily faster than XGB, although both can handle categorical features that are not already encoded. Thus, this investigation has considered CB-SHAP for constructing a CL structure based on an industrial copper flotation circuit dataset as an innovative approach. This work developed a *CL* to model a copper flotation plant (Delijan) to explore interactions in different conditions and highlight the most effective interactions within operational variables. Other typical machine learning methods such as random forest (RF), support regression machine (SVR), CNN, and XGB, which have been used recently for flotation modeling (Cook et al., 2020; Shahbazi et al., 2017; Y. Zhang et al., 2012), were also examined for comparison purposes.

2. Materials and methods

2.1. Dataset

A robust dataset was prepared from the Delijan copper flotation plant (Isfahan, Iran), which gathered daily data (2 shifts per day from 2021.03.21 to 2022.02.26) from monitored operational variables (Table 3). The dataset contains 684 records. The plant (Fig. 1) has two ball mills, and the flotation circuit has two parallel rougher flotation banks, one scavenger, and one cleaner bank. The plant capacity is 65 t/h with 0.5 % Cu content. Lime as a pH modifier and sodium silicate "SS" (Na_2SiO_3) as a depressant are added to the grinding circuit. pH is around 11.5 to 12, and the airflow rate is around 4000 m^3/h. Sodium isopropyl xanthate as an initial collector (SIPX), and Methyl Isobutyl Carbinol (MIBC) as a frother are added to the flotation circuit. Recovery and grade of concentrate are determined for the final products. From 2021.06.06, process engineers decided to substitute Sodium ethyl xanthate (SEX) as a secondary collector with Potassium amyl xanthate (PAX) since they assumed it is the most effective variable in the process efficiency. Thus, to assess such a hypothesis and explore variations after such a substitution, the dataset was split into two different conditions (SEX and PAX). Statistical assessments and *AI* modeling by various methods were considered for these two periods (datasets) to explore and compare operational variables' effectiveness levels, illustrate their interactions with the flotation responses (Cu recovery and Cu grade), and

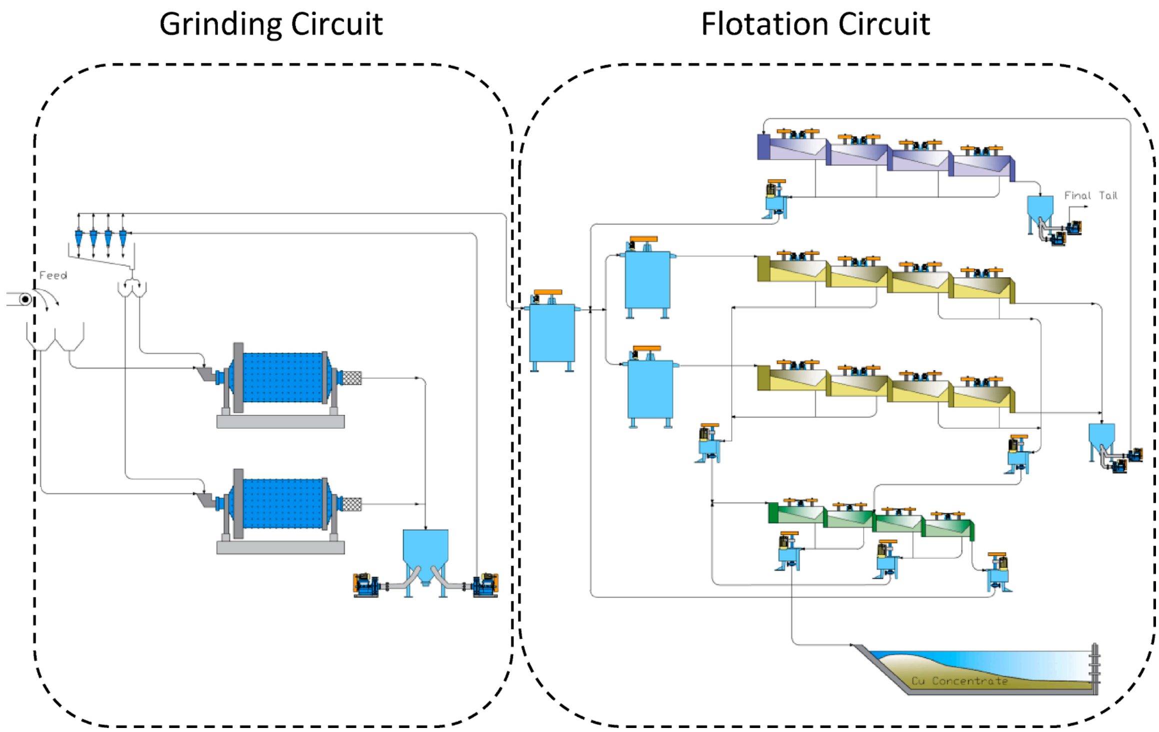

Fig. 1. The Delijan copper flotation flowsheet.

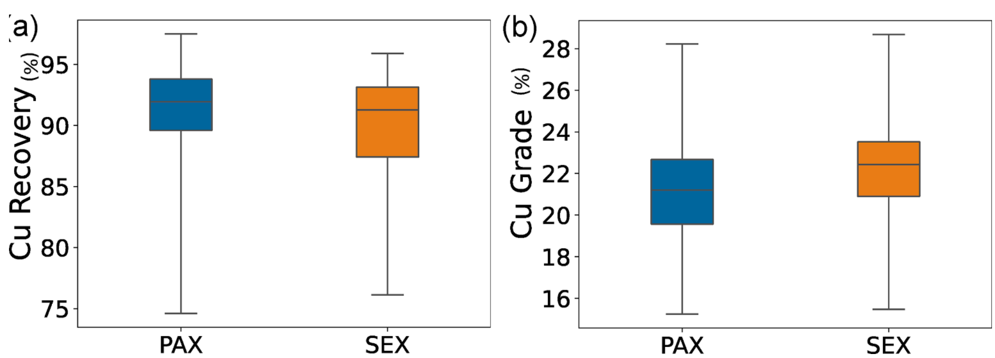

Fig. 2. A comparison between the flotation circuit's metallurgical responses in the presence of SEX and PAX.

rank them based on their importance.

After the secondary collector substitution, initial assessments of datasets indicated that changing SEX with PAX could increase recovery and slightly decrease the Cu grade in the plant products (Fig. 2). The higher recovery and lower grade of PAX versus SEX can be linked to the strength of PAX, which is much stronger in terms of collectivity and weaker in terms of selectivity than SEX (Ngobeni et al., 2013; Maree et al., 2017; T. Di Feo and Lastra, 2019; A. Di Feo et al., 2022). The representative metallurgical responses for both SEX and PAX periods were modeled using *AI* methods (CB, XGB, RF, SVR, and CNN) to find a robust construction for a *CL* dedicated to the Delijan copper flotation circuits. The most accurate model would be selected, and then the single (Pearson correlation) and multivariable interactions (SHAP) within operating variables will be assessed to rank variables based on their substantial effectiveness (SHAP) (Fig. 3).

2.2. *Intelligence*

2.2.1. *CatBoost*

CatBoost is a unique form of the gradient-boosting decision tree technique with robust learning capabilities for handling extremely nonlinear engine data (Deng et al., 2020). CatBoost is also renowned for needing less parameter adjustment, for its training speed, and for preventing overfitting more effectively than several previously published boosting models (Machado and Holmer, 2022). CatBoost estimates leaf values using a novel, efficient model that reduces overfitting (Jabeur et al., 2022). A novel technique is integrated to automatically convert categorical aspects as numerical characteristics, employing a mixture of category features that exploit the links between features, thereby significantly enhancing feature dimensions (Luo et al., 2021; Hussain et al., 2021). CatBoost can determine the relative importance of various features (i.e., the features utilized in the prediction) on the prediction result. The relative importance of a feature in a single decision tree is calculated as follows.

$$J_j^2 = \frac{1}{N\sum_{n=1}^{N} J_J^2(T_n)} \tag{1}$$

Here, N refers to the total number of trees or times the algorithm is run, and J_j^2 indicates how significant each feature is globally (Zeng et al., 2023). Ten variables (+149 μm, +74 μm, −74 μm, MIBC, PAX, SEX, SS, SIPX, Lime, Ball) were used to estimate the Cu grade and Cu recovery for

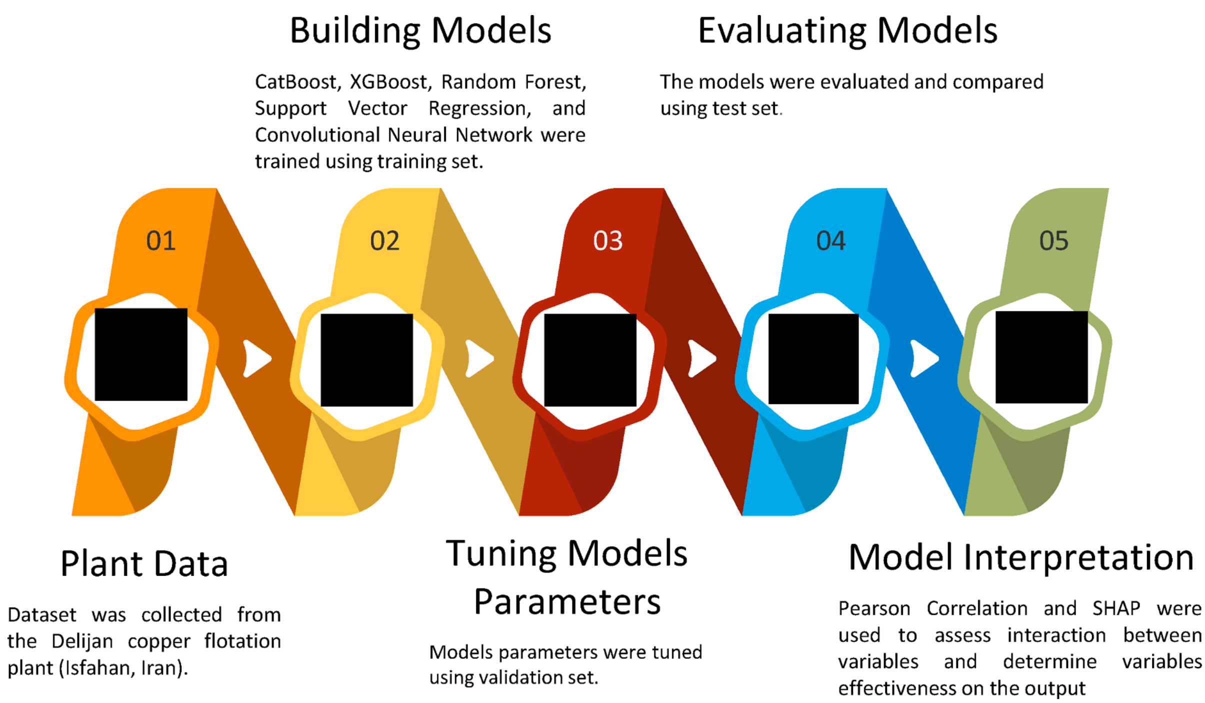

Fig. 3. The methodology was used for constructing the *CL*.

Table 4
The *AI* parameter settings for the predictive models.

Parameter	SEX		PAX	
	Cu grade	Cu recovery	Cu grade	Cu recovery
CatBoost				
Learning rate	0.20	0.29	0.35	0.10
Maximum number of trees	163	56	58	497
Maximum depth of trees	6	6	6	6
XGBoost				
Learning rate	0.40	0.80	0.10	0.19
Maximum number of trees	86	10	114	177
Maximum depth of trees	6	6	6	6
Random Forest				
Maximum number of trees	122	50	105	114
Maximum depth of trees	14	11	15	12
Support Vector Regression				
Kernel	Polynomial	Linear	Linear	Linear
Convolutional Neural Network				
Activation Function	Hyperbolic Tangent	Hyperbolic Tangent	Rectified Linear Unit	Sigmoid
Training Epochs	1000	1000	1000	1000
Batch Size	12	12	12	10

Table 5
Different AI models' outcomes (R^2) the prediction of metallurgical responses in various conditions.

Method		SEX		Pax	
		Validation	Test	Validation	Test
Cu grade	CB	0.90	0.90	0.84	0.80
	XGB	0.65	0.64	0.81	0.76
	RF	0.76	0.75	0.80	0.78
	SVR	0.05	0.27	0.41	0.46
	CNN	0.11	0.20	0.53	0.34
Cu recovery	CB	0.91	0.88	0.90	0.85
	XGB	0.81	0.80	0.79	0.77
	RF	0.87	0.87	0.79	0.78
	SVR	0.35	0.34	0.24	0.17
	CNN	0.66	0.40	0.14	0.15

both datasets, which significantly hindered the model's capacity to carry out sophisticated nonlinear regressions.

2.2.2. Extreme Gradient boosting

Extreme gradient boosting is known as XGBoost. Due to its fast learning and high accuracy, it has quickly risen to the ranks of the top ML algorithms. In recent years, XGBoost, a member of the boosting algorithm family, has been used in applied machine learning (Wang et al., 2022). It is optimized for speed and performance by implementing gradient-boosted decision trees. It alludes to the engineering aim of taxing the boundaries of computational resources in favor of boosted tree algorithms (Kardani et al., 2021).

Furthermore, XGBoost may stand to be a library of soft computing techniques that use both the new algorithm and GBDT techniques (Qiu et al., 2021; Sharma and Joshi, 2022). In the loss function of the XGBoost algorithm, the first-order Taylor expansion is used, whereas the GBDT algorithm uses the second-order Taylor expansion (Abbasniya et al., 2022). In addition, XGBoost normalizes the objective function to reduce the model's complexity and avoid overfitting (Nasiri and Hasani, 2022; Dong et al., 2023). Due to the high-depth complexity of the boosting tree approach, the resulting bias is low in mean and high in variation. In contrast, the random tree method's bias is high in mean and low in variance, indicating a greater capacity to match the training data (Bhati et al., 2021).

The objective function in the mth tree of the kth category is defined as follows:

$$Obj_{km} = L_{km} + \lambda_1 T_{km} + \frac{1}{2}\sum_{j=1}^{T_{km}}\left(\gamma_{jkm}^2\right) \quad (2)$$

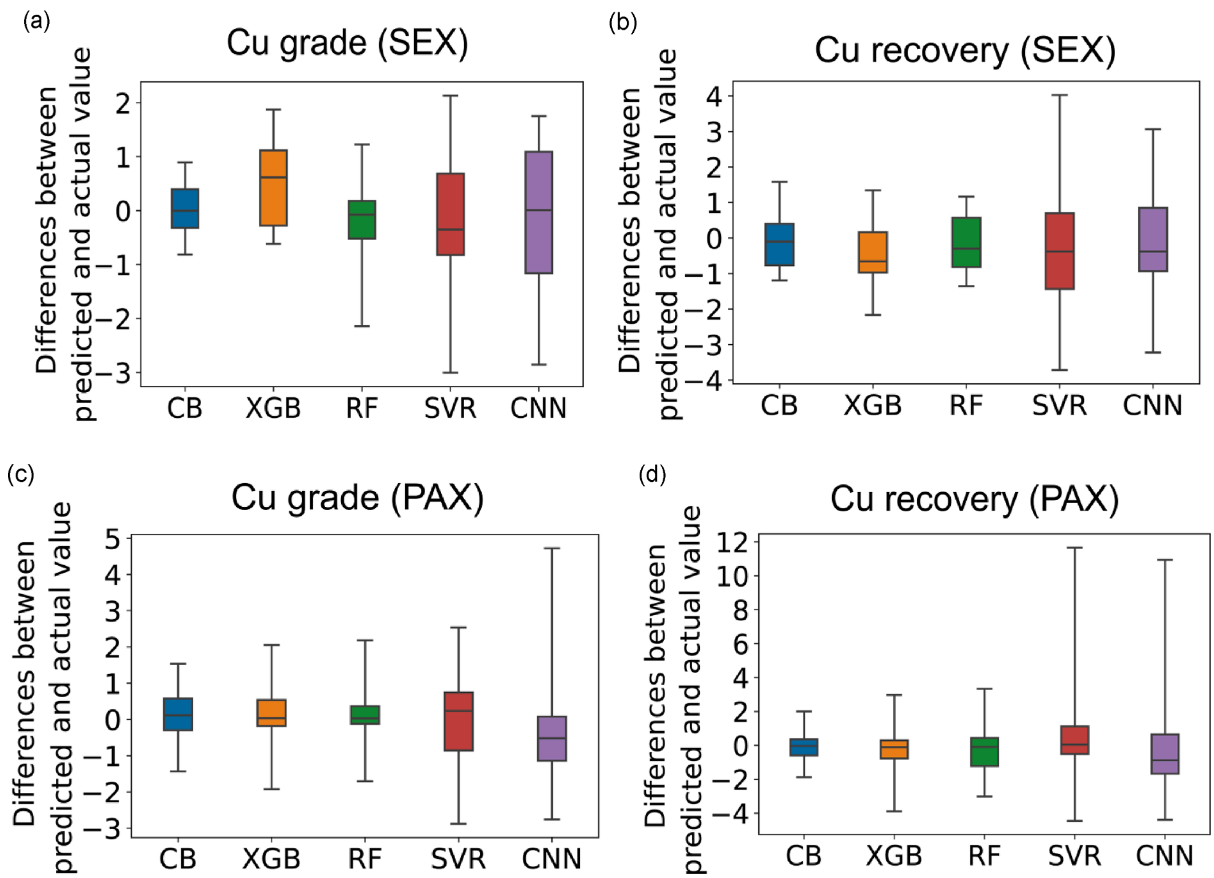

Fig. 4. Variation between actual and predicted metallurgical responses for different conditions.

where λ_1 is the leaf node number and T_{km} denotes the number of leaf nodes in the first m or mth trees (Chelgani et al., 2021a; Dezhkam and Manzuri, 2023).

2.2.3. Random Forest

Random Forest (RF) is an unsupervised machine-learning technique (Homafar et al., 2022). RF is a statistical learning theory that uses the bootstrap resampling technique to extract numerous samples from the original sample, build the decision tree for each bootstrap sample, and then integrate the average forecasts of multiple decision trees to provide the final forecast results (W. Zhang et al., 2021; Chen et al., 2023). RF is a flexible ensemble approach that can accommodate missing data, eliminates overfitting, is resilient to outliers, and provides an unbiased estimate of the generalization error (Nasiri et al., 2021; Fatimah et al., 2022). It constructs and combines many decision trees for more accurate and consistent predictions (Palimkar et al., 2022). Scale invariance and a few tunable parameters are benefits of RF modeling (Tohry et al., 2020). In a formal sense, the RF model's anticipated output $\widehat{\tau}(x)$ may be calculated as follows, given an input feature vector x $= [x_1, x_2, \ldots, x_n]^T$:

$$\tau(x) = \frac{1}{B}\sum_{b=1}^{B}\widehat{\tau}_b(x) \tag{3}$$

where $\widehat{\tau}_b(x)$ is the estimate produced by the bth tree and B is the total number of trees.

2.2.4. Support vector regression

SVR is a well-known MLA created using Vapnik's idea (1995). The modeling and regulation of intricate engineering systems are the primary applications of this technique (Panahi et al., 2020). Regression issues were addressed by developing the SVR technique based on the SVM approach (Paryani et al., 2022). SVR can learn nonlinear relationships in the data, has a good generalization capacity and requires no knowledge of the input space dimension for its computational complexity (Nasiri et al., 2021). In addition, it offers a high degree of predictive accuracy and wide application. Instead of reducing the error during training, SVR prioritizes doing it in a way that will have the most negligible impact on generalization. The SVR uses the following equation to tackle the regression issue.

$$f(x) = \langle w\varphi(x)\rangle + b \tag{4}$$

where $\varphi(x)$ represents the multidimensional space containing the input vector x, w stands for the matrix's weight, and b stands for the bias (Fatahi et al., 2023; Homafar et al., 2022).

2.2.5. Convolutional Neural networks

LeCun et al. (LeCun et al., 1998) presented the first widely-used convolutional neural network (CNN) for recognizing handwriting. Throughout the last few decades, numerous extremely robust networks have accomplished unprecedented success on massive image classification tasks (Guo et al., 2022). In image understanding, which includes classification, segmentation, localization, detection, etc., CNN offers a revolutionary leap forward. CNNs' effectiveness in image understanding is the primary reason for their widespread adoption (Sarvamangala and Kulkarni, 2022). Theoretically, CNNs have been demonstrated to be universal approximators that can estimate any nonlinear function to any desired accuracy (Nasiri and Ebadzadeh, 2022). Two of CNN's unique characteristics that contribute to its enormous success are sparse connection and shared weights (Huo et al., 2021). Mathematically speaking, for a fully connected layer of CNN the following calculation takes place:

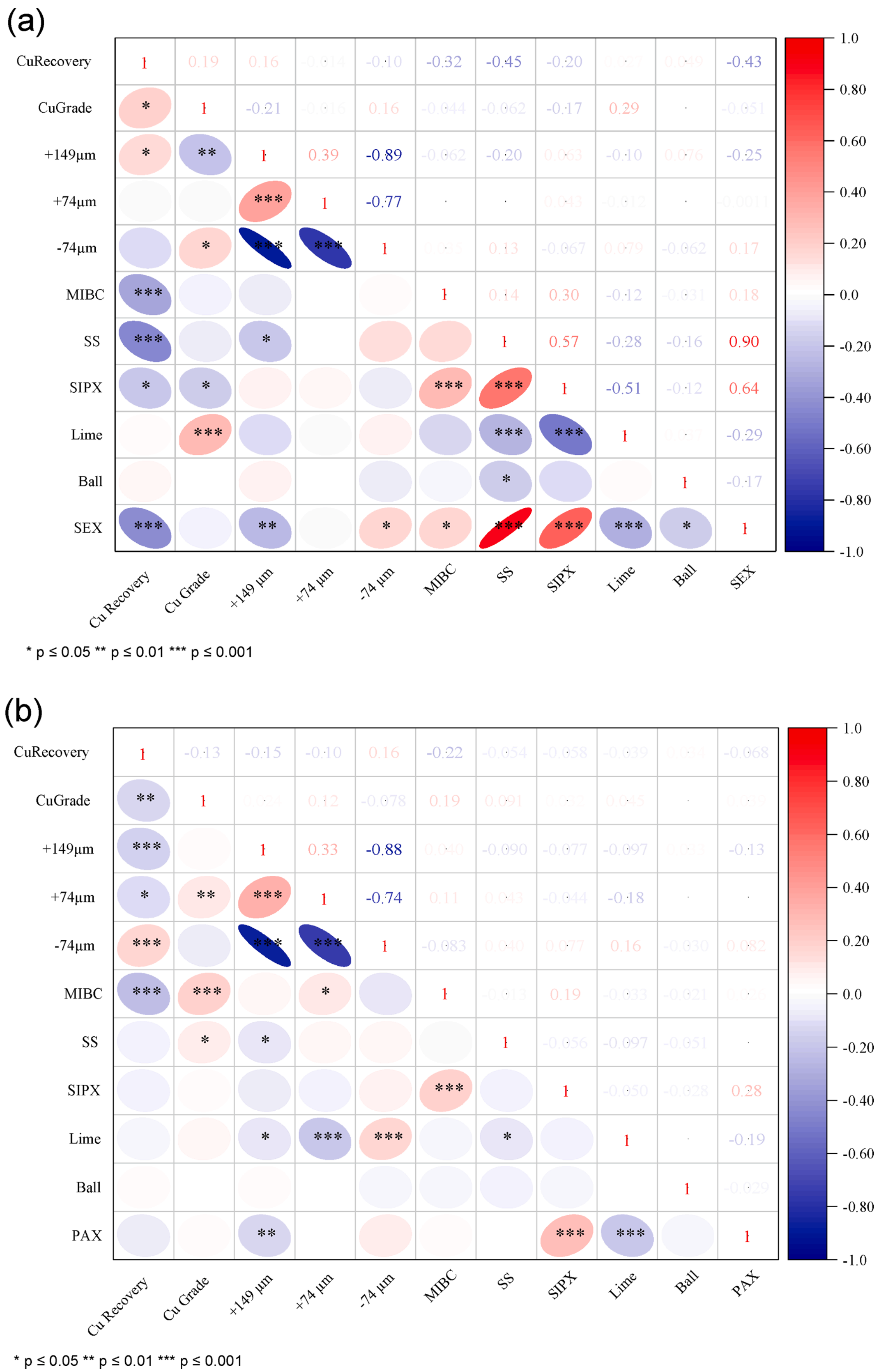

Fig. 5. Pearson correlation assessments in different conditions (a) SEX collector, (b) PAX collector.

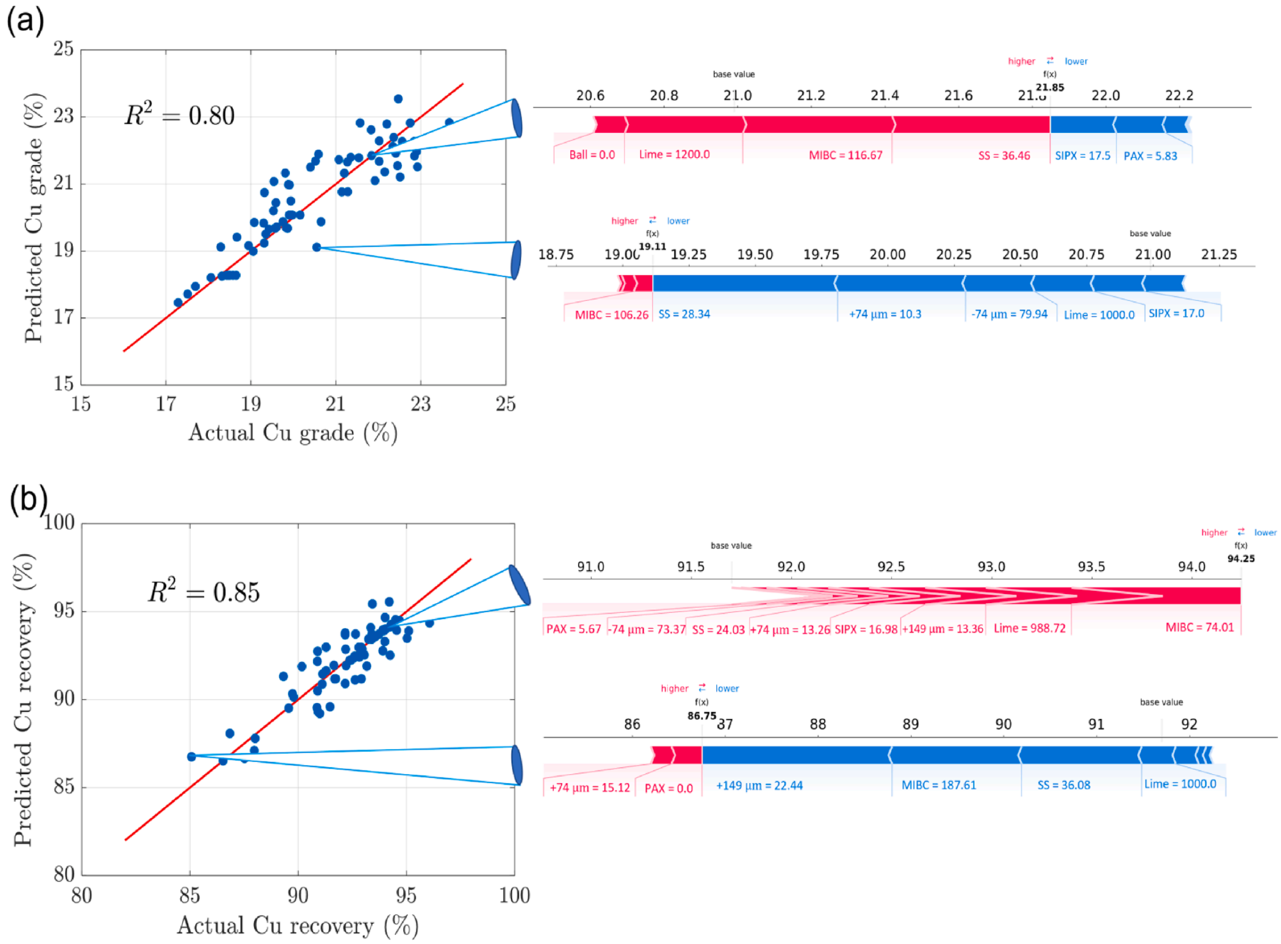

Fig. 6. The possibility of SHAP analyses for each record of the CB model outcomes when the secondary collector was PAX.

$$y = f\left(\sum_i w_i x_i + b\right) \tag{5}$$

where x denotes the input vector, w is the weight vector, b represents the bias vector, $f(.)$ is the activation function, and y denotes the output.

2.2.6. Shapley additive explanations

Lundberg and Lee introduced the Shapley Additive Explanations (SHAP) value, a vital component of any EAI model (Chelgani et al., 2021a). SHAP is a framework based on game theory that offers a consistent method for understanding machine learning model predictions and assigning feature priority to input variables (Chelgani et al., 2021b). It is possible to utilize it in combination with a variety of ML models in order to understand the models (X. Wen et al., 2021a). The game payout serves as the forecast in the context of predictive analytics, while the players themselves serve as the variables. Calculating Shapley values ensures an equitable division of the final forecast among the values of the collection of variables (Vaulet et al., 2022). It becomes computationally expensive to calculate the marginal contribution of predictors as the number of predictor variables grows since the number of combinations of predictor variables grows exponentially. SHAP values can circumvent this constraint since sample approximations make their calculation more efficient. Nonetheless, they still maintain the features of Shapley's values. To be more precise, the SHAP value of a feature is the difference between the average prediction value of the samples that include this feature and the average prediction value of the other samples that do not (Kang et al., 2022).

Shapley values have three natural qualities that show the direction in which features have an impact on the model: their local correctness (also known as additivity), consistency (also known as symmetry), and nonexistence (also known as null effect) (Jones et al., 2022; Liang et al., 2022; Zhou et al., 2021). Consequently, we may define the explanatory model, $g(z')$, as follows:

$$g(z') = \phi_0 + \sum_{i=1}^{M} \phi_i z'_i \tag{6}$$

where M is the total number of features in the dataset, and $\boldsymbol{z}'$ is the vector of input variables simplified from the original dataset's $\boldsymbol{z}$. ϕ_0 is a constant used when all inputs are null, and ϕ_i is the attribute value for each feature (Feng et al., 2021). When a model f is provided, the equation that may be used to calculate the Shapley values ϕ_i for each input feature is as follows:

$$\phi_i = \sum_{S \in N \setminus \{i\}} \frac{|S|!(|N| - |S| - 1)!}{|N|!} [V(S \cup \{x_i\}) - V(S)] \tag{7}$$

where N represents the set of all variables and S represents a subset of N (Nasiri et al., 2021).

3. Results and discussions

3.1. Metallurgical responses' prediction

Records from the plant' datasets were randomly split into 70, 15, 15 % for training, validation, and testing of the *AI* models for the metallurgical responses' predictions. Different features were examined for each model to find the optimum hyperparameter values to adjust and

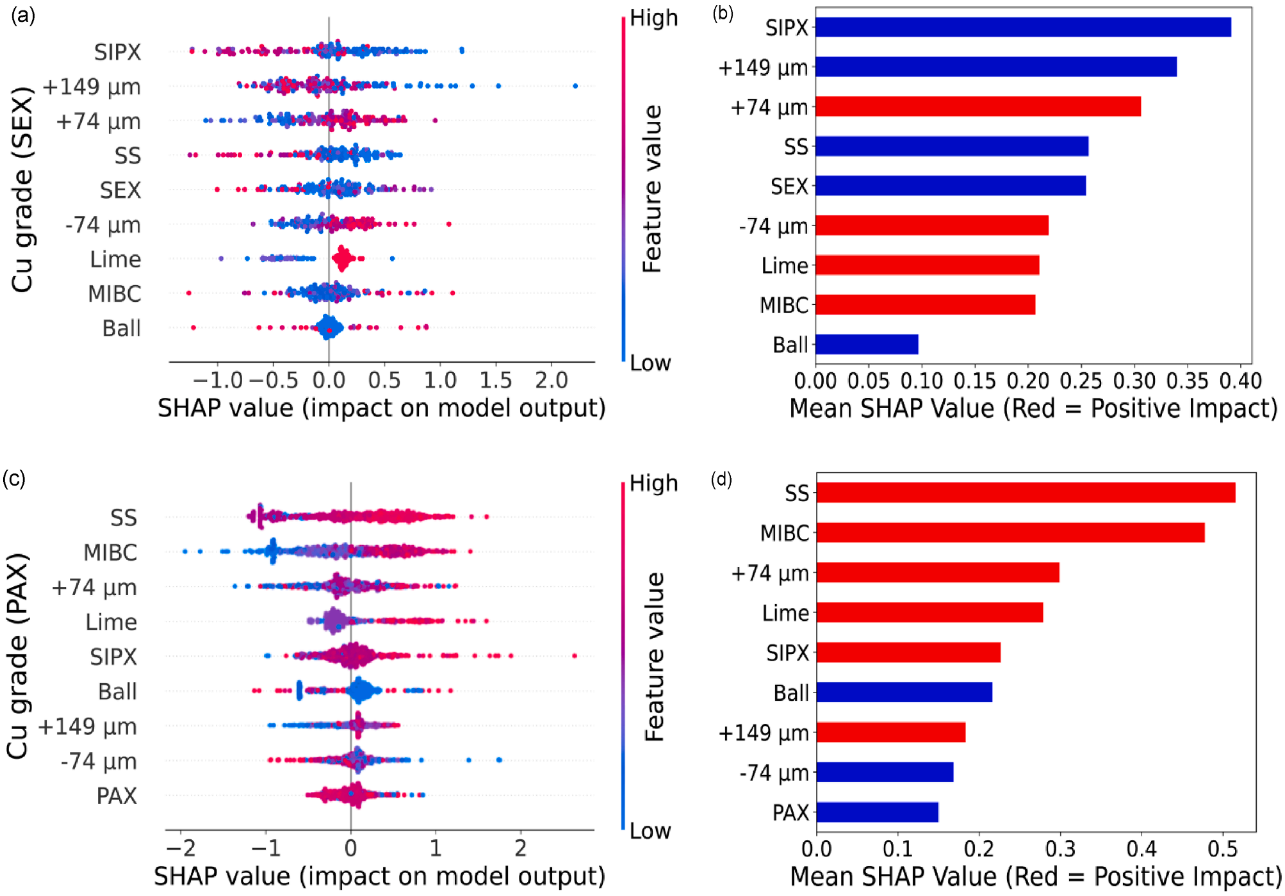

Fig. 7. SHAP values and ranking variable effectiveness on Cu grade (a-b) SEX collector and (c-d) PAX collector.

tune them for the training stage (a try-and-error system) (Table 4). The *AI* outcomes, apart from the model type (Table 5), indicated that the predictability of Cu recovery decreased by changing the secondary collector on the plant from SEX to PAX. Based on *AI* results in the validation and testing stages, CB model could accurately estimate the flotation metallurgical responses based on the plant's operational variables (Table 5). CB outcomes illustrated the lowest error in comparison with other models (Fig. 4). The absolute value of errors between actual and CB-predicted metallurgical responses indicated for both collectors "SEX" and "PAX" the maximum difference was less than 2 % (Fig. 4).

The highest CB prediction accuracy could have different reasons. RF is a bagging method, whereas XGBoost and CatBoost are boosting techniques requiring less feature engineering (Homafar et al., 2022). CNN can learn complicated nonlinear interactions but requires multiple fine-tuning parameters and designing its structure. It also needs a lot of training samples to learn network weights effectively. SVR is limited by selecting an appropriate kernel function. XGB is susceptible to gradient boosting bias and prediction shift; however, CatBoost overcomes these issues by using the ordered boosting technique. CB surpassed other ML algorithms when it came to the regression problem, as evidenced by earlier research findings (Gao et al., 2022; Luo et al., 2021; Bentéjac et al., 2021; Ibrahim et al., 2020).

3.2. Intercorrelations

3.2.1. Pearson correlation

Interaction assessments by Pearson correlation indicated that in the plant' steady-state process conditions, none of the operating variables had a significant single linear correlation ($|r| \leq 0.7$) (Shahbazi et al., 2013) with the metallurgical responses (Cu recovery and grade (Fig. 5)). SEX concentration (Fig. 5a) had negative correlations with recovery (r: −0.43: means increasing SEX concentration led to a decrease of the Cu recovery) and no considerable effect on the Cu grade. When the secondary collector was changed by PAX (Fig. 5b), PAX concentration did not show any substantial linear effectiveness on the metallurgical responses of the flotation. As mentioned, PAX has low selectivity and is mostly used in the scavenger stage of the sulfide flotation circuit. Its long alkyl chain enhanced its collecting power (potentially should increase recovery) (Botero et al., 2022). However, linear assessments showed that the secondary collector concentration would not be the most effective parameter on the process responses, and the substitution of SEX with PAX did not provide a remarkable process improvement. Maree et al. (2017) indicated that using various xanthate collector mixtures is mostly beneficial in mass and water recovery (not based on metals' recovery and grade) (Maree et al., 2017).

Pearson correlation indicated (Fig. 5) that by substitution of the secondary collector (PAX instead of SEX), the sub-interactions within the plant's monitored variables were changed. In the presence of SEX, Cu grade showed a negligible positive correlation with Cu recovery (r: 0.19). Since PAX was used in the plant, this relationship reversed to a slight negative correlation (r: −0.13). Such a relationship is quite understandable since, generally, by increasing the cumulative recovery after a certain point, the cumulative grade decreases (negative correlation between recovery and grade) (Neethling and Cilliers, 2012; Wills and Finch, 2015). In the presence of SEX, SS concentration has the highest negative linear correlation with Cu recovery (r: −0.45); however, when PAX was used, SS concentration had a negligible relationship with Cu recovery (r: ~0). SEX and SS concentration illustrated a significant positive linear correlation; thus, it could be statistically the reason that by increasing their concentrations, the recoveries were decreased (Fig. 5a). Lime concentration showed no linear effect on the recovery, though it had the highest positive interaction with Cu grade (r:

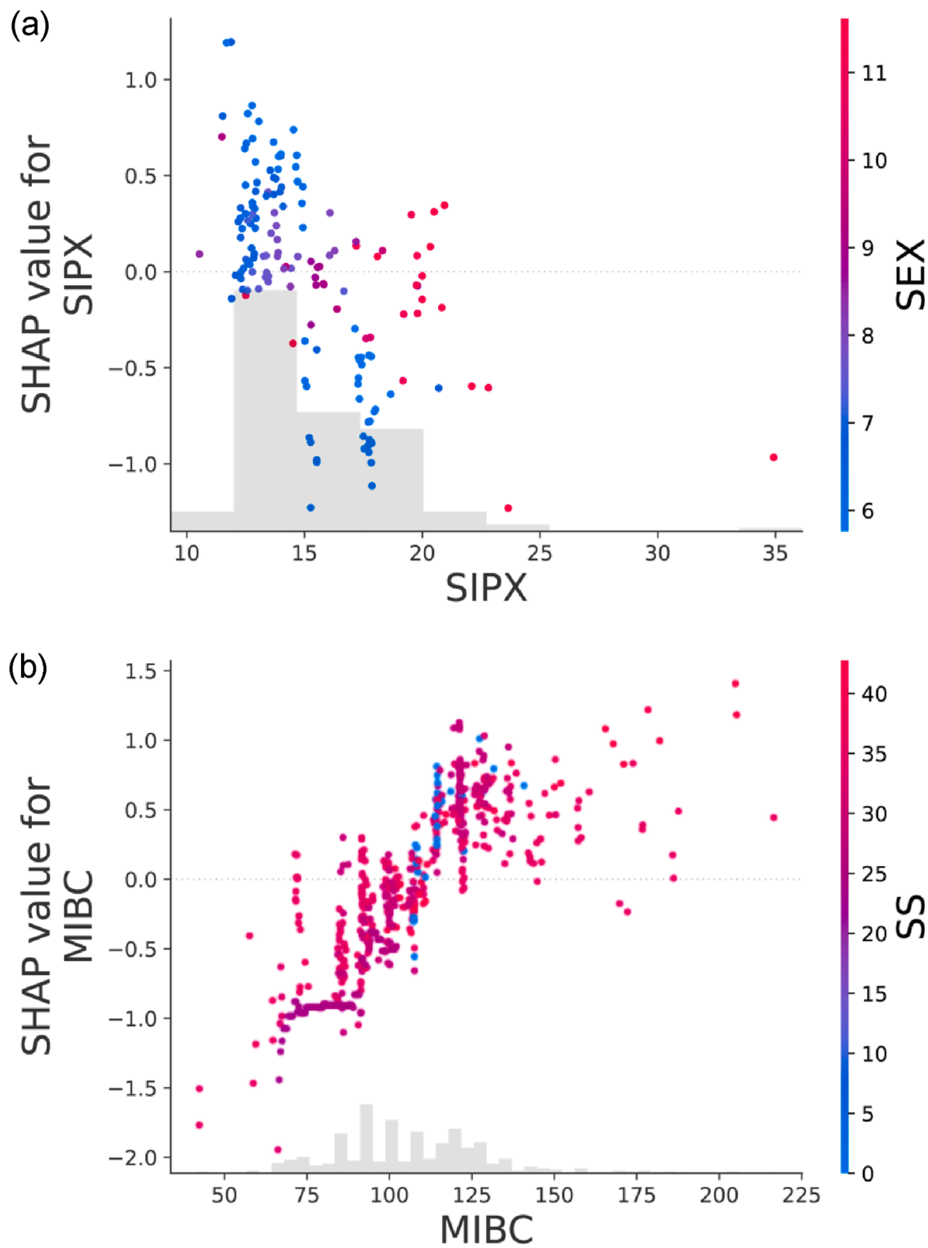

Fig. 8. Interaction of various variables in different conditions and their effects on the Cu grade.

0.29) when the plant ran with SEX. However, by PAX substation, it showed no linear correlation with Cu grade. MIBC concentration had the highest positive linear correlation (r: 0.19) with Cu grade and the highest negative relationship with Cu recovery when PAX was used as the secondary collector. The particle size effectiveness pattern also completely changed when PAX replaced SEX. The positive linear correlation of + 149 μm fraction on the Cu recovery change from r: 0.16 to −0.15. These results can be linked to PAX's lower selectivity and higher collectivity than SEX (Ngobeni et al., 2013; Maree et al., 2017; T. Di Feo and Lastra, 2019; A. Di Feo et al., 2022). These results indicated that by substituting only one secondary flotation reagent in the plant, the whole relationship networks could be changed, and single linear assessments cannot fully address all the potential interactions. These variations emphasized the importance of SHAP multivariable correlation assessments (would be led to rank variables based on their effectiveness and find the most significant one).

3.2.2. SHAP

SHAP (multivariable linear-nonlinear) can explore and determine the effectiveness of all multivariable correlations for each record through the modeling and illustrate how each record can interact with the model outcomes and prediction results (Fig. 6). However, SHAP value as an average of all interactions of each variable based on all the records can illustrate the multi correlations.

SHAP assessments illustrated (Figs. 7 and 9) that the type of secondary collector (SEX or PAX) in the process was not essential for the flotation metallurgical responses. The concentration of both secondary collectors showed a negative correlation magnitude with the process metallurgical responses (Figs. 7 and 9). After a certain concentration of these collectors, a decrease in metallurgical responses was reported in other investigations (Güler, 2012; Mokgethwa et al., 2016; Tapley and Yan, 2003). Tapley and Yan (2003) documented that after 3.21 × 10^{-3} mol/l SEX, the recoveries of arsenopyrite and pyrite (as sulfides) were dropped (Tapley and Yan, 2003). Asadi et al. (2019) reported that increasing PAX (40 to 100 g/t) as the main collector would increase the

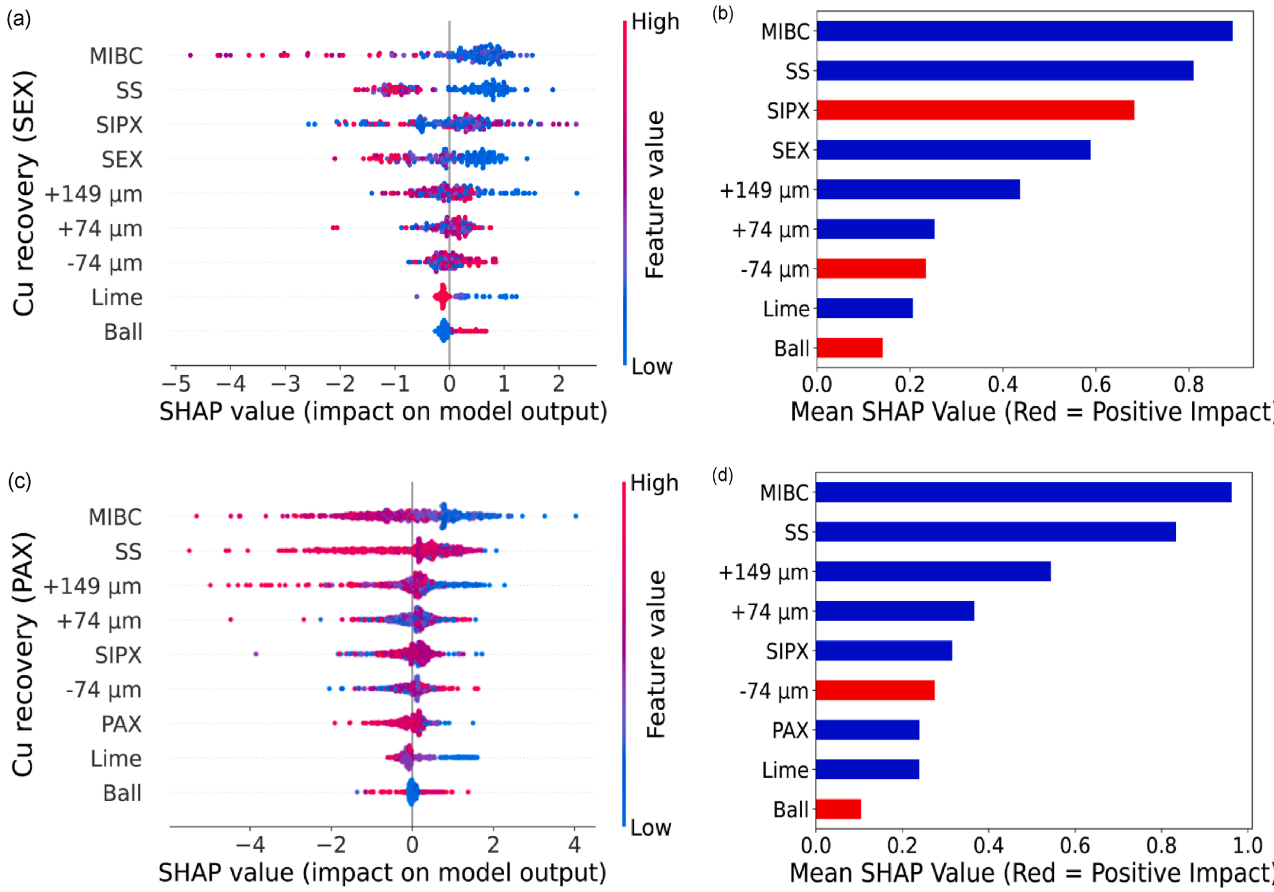

Fig. 9. SHAP values and ranking variable effectiveness on Cu recovery (a-b) SEX collector, and (c-d) PAX collector.

Cu recovery and decrease the Cu grade (Asadi et al., 2019).

However, substituting the secondary collector changed the multi-interactions (as also observed in the linear assessments). Based on the SHAP results (Fig. 7a), when SEX was used as the secondary collector in the plant, the most influential variable on the Cu grade was the initial collector concentration (SIPX). This effectiveness was negative on average (Fig. 7b). SHAP interactions indicated (Fig. 8a) that the efficacy of SIPX and SEX concentrations was positive on Cu grade when simultaneously their dosages were 12.5–15 and 6–7 g/t, respectively. The second most effective variable on the Cu grade was the mass percentage of coarse particle fraction (+149 µm). The nature of this negative effect is evident since mineral liberation mostly happens in the lower size fraction. It was reported that SEX collectivity power is much more suitable for narrow particle size distribution, and it can mostly deal with coarse particles, while PAX collectivity with higher molecular weight is higher and can float a wider range of particles (less selective) (Wood, 1972). Di Feo and Lastra (2019) showed the collectivity of SEX for + 150 µm was two times higher than PAX through Cu and molybdenite flotation (T. Di Feo and Lastra, 2019). Therefore, the importance of particle size could be leveled down in the presence of PAX. Lime had a positive correlation apart from conditions on the Cu grade. It was well understood that lime could modify the process pH, and its calcium cation can also act as a depressant for pyrite and enhance Cu grade (Fig. 7), while it may adversely affect the recovery (Fig. 9) (Zanin et al., 2019; Tikka, 2014).

In the PAX presence, SS had the highest effectiveness (positive) on the Cu grade (Fig. 7c). It was reported that SS in a certain concentration has a positive effect on Cu grade and can improve it; however, after that dosage may decrease recovery (Ramirez et al., 2018; Rabatho et al., 2011). While, SS had the highest importance (negative) with Cu recovery (Fig. 9c–d). In general, the substitution of SEX by PAX did not change the ranking of the most effective operational variables on Cu recovery (Fig. 9d). Li et al. (2019) reported that SS could reduce precipitation of hydrophilic $Mg(OH)_2$ on chalcopyrite surface improve process selectivity (Li et al., 2019). Asadi et al. (2019) also reported that in the presence of PAX, by increasing SS concentration, Cu grade increased, and its recovery decreased when SS was over 1200 g/t (Asadi et al., 2019). However, Muanda et al. (2021) showed that by increasing SS concentration (200 to 500 g/t) in the presence of PAX, Cu grade and recovery could be quite varied, and on average, both would be decreased (Muanda et al., 2021). By using PAX, the importance of MIBC on Cu grade markedly enhanced (Fig. 7c). Pan et al. (2022a) indicated that the MIBC foaminess could be drastically changed in the presence of PAX, and even its low concentration in the pulp could particularly increase the MIBC foaminess (Pan et al., 2022b). PAX would adsorb at the air–liquid interface at high concentrations, increase the MIBC adsorption (Pan et al., 2021), and improve the bubble stability (Pan et al., 2022b). Increasing MIBC (over 125 g/t) even in lower SS concentrations could enhance the Cu grade in the plant when PAX was the secondary collector (Fig. 8b). These outcomes would confirm that SHAP-CB can profitably construct a *CL* for modeling metallurgical responses of the plant and illustrating multi-interactions. Such an accurate structure hypothetically portrayed that this approach could be used for monitoring, maintaining, and optimizing similar circuits and educating operators.

4. Conclusion

Froth flotation, as the most known efficient technique, has been used to process low-grade critical raw materials. Since flotation separation deals with several subprocesses, its modeling is quite complicated on the industrial scale. As an innovative AI concept, a conscious lab can be used to explain these complex relationships within the industrial datasets and predict potential flotation metallurgical responses (grade and recovery). This study constructed a conscious lab based on SHAP, one of the most recently released *XAI* systems. Multivariable relationship assessments by SHAP highlighted that substituting SEX as a secondary collector with PAX decreased the level of secondary collector importance on the metallurgical responses (Cu grade and recovery). In general, by increasing the concentration of the secondary collector, the process efficiency was decreased for both SEX and PAX (negative interaction). SHAP outcomes indicated that substituting SEX by PAX could change all interactions within the processing parameters. These variations mostly altered the interactions between flotation operational variables and the Cu grade. *AI* modeling with various methods indicated that Catboost, as a novel system, could accurately predict metallurgical responses. The Catboost outcomes represented higher accuracy than other known machine learning (support vector regression, random forest, and XGBoost) and convolutional neural network methods. The Catboost prediction errors for both recovery and grade were lower than 2 %. *AI* modeling results also indicated that the secondary collector substitution generally reduced process predictability (R^2: ~0.90 s vs. ~ 0.80 s). The main outcomes of this investigation indicated that using an advanced explainable *AI* system, "Catboost-SHAP," for constructing a conscious lab could lead to understanding interactions within monitoring variables on the industrial plants, train operators, predict product quality, and enhance process efficiency.

Ethics approval

Not applicable.

CRediT authorship contribution statement

Saeed Chehreh Chelgani: Writing – review & editing, Writing – original draft, Visualization, Supervision, Methodology, Investigation, Funding acquisition, Data curation, Conceptualization. **Arman Homafar:** Software, Formal analysis, Data curation. **Hamid Nasiri:** Writing – original draft, Software, Methodology, Data curation. **Mojtaba Rezaei laksar:** Resources, Data curation.

Declaration of competing interest

The authors declare that they have no known competing financial interests or personal relationships that could have appeared to influence the work reported in this paper.

Data availability

Data will be made available on request.

Acknowledgements

This manuscript resulted from a project financially supported by CAMM3, the Center of Advanced Mining and Metallurgy, a center of excellence at the Luleå University of Technology, Sweden and by WISE-WASP project.

References

Abbasniya, M.R., Sheikholeslamzadeh, S.A., Nasiri, H., Emami, S., 2022. Classification of breast tumors based on histopathology images using deep features and ensemble of gradient boosting methods. Comput. Electr. Eng. 103, 108382 https://doi.org/10.1016/j.compeleceng.2022.108382.

Abdulhussein, S.A.A., Alwared, A.I., 2019. The Use of Artificial Neural Network (ANN) for Modeling of Cu (II) Ion Removal from Aqueous Solution by Flotation and Sorptive Flotation Process. Environ. Technol. Innov. 13. Elsevier, 353–363.

Ai, M., Xie, Y., Xie, S., Li, F., Gui, W., 2019. Data-Driven-Based Adaptive Fuzzy Neural Network Control for the Antimony Flotation Plant. J. Franklin Inst. 356 (12). Elsevier, 5944–5960.

Alidokht, Mehdi, Yazdani, Samaneh, Hadavandi, Esmaeil, Chelgani, Saeed Chehreh, 2021. Modeling Metallurgical Responses of Coal Tri-Flo Separators by a Novel BNN: A 'Conscious-Lab' Development. Int. J. Coal Sci. Technol. 8 (6), 1436–1446. Springer.

Al-Thyabat, S., 2009. Investigating the Effect of Some Operating Parameters on Phosphate Flotation Kinetics by Neural Network. Adv. Powder Technol. 20 (4). Elsevier, 355–360.

Asadi, M., Soltani, F., Mohammadi, M.R.T., Khodadadi, D.A., Abdollahy, M., 2019. A Successful Operational Initiative in Copper Oxide Flotation: Sequential Sulphidisation-Flotation Technique. Physicochemical Problems of Mineral Processing 55.

Bai, Y., Wang, Y., Zeng, Y., Jiang, Y., Xia, S.-T., 2023. Query Efficient Black-Box Adversarial Attack on Deep Neural Networks. Elsevier:, p. 109037. Pattern Recognition 133.

Bentéjac, Candice, CsörgHo, Anna, Mart'inez-Muñoz, Gonzalo, 2021. A Comparative Analysis of Gradient Boosting Algorithms. Artificial Intell. Rev. 54 (3), 1937–1967. Springer.

Bhati, Bhoopesh Singh, Garvit Chugh, Fadi Al-Turjman, and Nitesh Singh Bhati. 2021. "An Improved Ensemble Based Intrusion Detection Technique Using XGBoost." Transactions on Emerging Telecommunications Technologies 32 (6). Wiley Online Library: e4076.

Botero, Y.L., Canales-Mahuzier, A., Serna-Guerrero, R., López-Valdivieso, A., Benzaazoua, M., Cisternas, L.A., 2022. Physical-Chemical Study of IPETC and PAX Collector's Adsorption on Covellite Surface. Appl. Surf. Sci. 602. Elsevier, 154232.

Chelgani, S.C., 2021. Estimation of Gross Calorific Value Based on Coal Analysis Using an Explainable Artificial Intelligence. Machine Learning with Applications 6. Elsevier: 100116.

Chelgani, Saeed Chehreh, Behzad Shahbazi, and Bahram Rezai. 2010. "Estimation of Froth Flotation Recovery and Collision Probability Based on Operational Parameters Using an Artificial Neural Network." International Journal of Minerals, Metallurgy, and Materials 17 (5). Springer: 526–534.

Chelgani, S.C., Nasiri, H., Alidokht, M., 2021b. Interpretable Modeling of Metallurgical Responses for an Industrial Coal Column Flotation Circuit by XGBoost and SHAP-A 'Conscious-Lab' Development. Int. J. Min. Sci. Technol. 31 (6). Elsevier, 1135–1144. https://doi.org/10.1016/j.ijmst.2021.10.006.

Chelgani, C., Saeed, H.N., Tohry, A., 2021a. Modeling of Particle Sizes for Industrial HPGR Products by a Unique Explainable AI Tool- A 'Conscious Lab' Development. Adv. Powder Technol. 32 (11). Elsevier, 4141–4148. https://doi.org/10.1016/j.apt.2021.09.020.

Chelgani, C., Saeed, H.N., Tohry, A., Heidari, H.R., 2023. Modeling Industrial Hydrocyclone Operational Variables by SHAP-CatBoost - A 'Conscious Lab' Approach. Powder Technol. 420. Elsevier, 118416 https://doi.org/10.1016/j.powtec.2023.118416.

Chen, S., Yang, R., Zhong, M., Xi, X., Liu, C., 2023. A Random Forest and Model-Based Hybrid Method of Fault Diagnosis for Satellite Attitude Control Systems. IEEE, IEEE Transactions on Instrumentation and Measurement.

Cook, Rachel, Keitumetse Cathrine Monyake, Muhammad Badar Hayat, Aditya Kumar, and Lana Alagha. 2020. "Prediction of Flotation Efficiency of Metal Sulfides Using an Original Hybrid Machine Learning Model." Engineering Reports 2 (6). Wiley Online Library: e12167.

Deng, K., Zhang, X., Cheng, Y., Zhiyong Zheng, Fu., Jiang, W.L., Peng, J., 2020. A Remaining Useful Life Prediction Method with Long-Short Term Feature Processing for Aircraft Engines. Appl. Soft Comput. 93. Elsevier, 106344.

Dezhkam, A., Manzuri, M.T., 2023. Forecasting Stock Market for an Efficient Portfolio by Combining XGBoost and Hilbert–Huang Transform. Eng. Appl. Artif. Intel. 118. Elsevier: 105626 https://doi.org/10.1016/j.engappai.2022.105626.

Di Feo, A, M De Souza, R Lastra, and A Hobert. 2022. "Effect of Strong Collectors and Frothers on Coarse Particle Flotation Using the HydroFloat™ for a North American Concentrator." CIM Journal 13 (3). Taylor \& Francis: 107–124.

Dong, J., Zeng, W., Lifeng, Wu., Huang, J., Gaiser, T., Srivastava, A.K., 2023. Enhancing Short-Term Forecasting of Daily Precipitation Using Numerical Weather Prediction Bias Correcting with XGBoost in Different Regions of China. Eng. Appl. Artif. Intel. 117. Elsevier: 105579.

Fatahi, Rasoul, Rasoul Khosravi, Hossein Siavoshi, Samaneh Yazdani, Esmaiel Hadavandi, and Saeed Chehreh Chelgani. 2021. "Ventilation Prediction for an Industrial Cement Raw Ball Mill by BNN—A 'Conscious Lab' Approach." *Materials* 14 (12). Multidisciplinary Digital Publishing Institute: 3220.

Fatahi, Rasoul, Hamid Nasiri, Ehsan Dadfar, and Saeed Chehreh Chelgani. 2022. "Modeling of Energy Consumption Factors for an Industrial Cement Vertical Roller Mill by SHAP-XGBoost: A 'Conscious Lab' Approach." *Scientific Reports* 12 (1). Nature Publishing Group: 7543. doi:10.1038/s41598-022-11429-9.

Fatahi, Rasoul, Hamid Nasiri, Arman Homafar, Rasoul Khosravi, Hossein Siavoshi, and Saeed Chehreh Chelgani. 2023. "Modeling Operational Cement Rotary Kiln Variables with Explainable Artificial Intelligence Methods – a 'Conscious Lab' Development." *Particulate Science and Technology* 41 (5). Taylor \& Francis: 715–724. doi:10.1080/02726351.2022.2135470.

Fatimah, B., Singh, P., Singhal, A., Pachori, R.B., 2022. Biometric Identification From ECG Signals Using Fourier Decomposition and Machine Learning. IEEE Trans. Instrum. Meas. 71. IEEE, 1–9.

Feng, De-Cheng, Wen-Jie Wang, Sujith Mangalathu, and Ertugrul Taciroglu. 2021. "Interpretable XGBoost-SHAP Machine-Learning Model for Shear Strength Prediction of Squat RC Walls." *Journal of Structural Engineering* 147 (11). American Society of Civil Engineers: 4021173.

Di Feo, Tony, and Rolando Lastra. 2019. "Effects of Collectors and Frothers on Copper and Molybdenum Coarse Particle Recoveries—A Statistical Approach." Journal of

Minerals and Materials Characterization and Engineering 7 (3). Scientific Research Publishing: 117–136.
Fu, Y., Aldrich, C., 2018. Using Convolutional Neural Networks to Develop State-of-the-Art Flotation Froth Image Sensors. IFAC-PapersOnLine 51 (21). Elsevier, 152–157.
Fu, Y., Aldrich, C., 2019. Flotation Froth Image Recognition with Convolutional Neural Networks. Miner. Eng. 132. Elsevier, 183–190.
Gao, W., Zhou, L., Liu, S., Guan, Y., Gao, H., Jianjun, Hu., 2022. Machine Learning Algorithms for Rapid Estimation of Holocellulose Content of Poplar Clones Based on Raman Spectroscopy. Elsevier, Carbohydrate Polymers, p. 119635.
Ghaffari, Ali, Mohammad Hayati, and Arash Shekholeslami. 2012. "Probability and Sensitivity Analysis in Flotation Circuit of Bama Lead and Zinc Processing Plant Using Monte Carlo Simulation Method." *Mineral Processing and Extractive Metallurgy Review* 33 (6). Taylor \& Francis: 416–426.
Güler, E. 2012. "Bulk Flotation of Low Grade Refractory Sulfide Lead-Zinc Ore." *Asian Journal of Chemistry* 24 (2). Asian Journal of Chemistry: 499.
Guo, Jianyuan, Kai Han, Han Wu, Yehui Tang, Xinghao Chen, Yunhe Wang, and Chang Xu. 2022. "Cmt: Convolutional Neural Networks Meet Vision Transformers." In Proceedings of the IEEE/CVF Conference on Computer Vision and Pattern Recognition, 12175–12185.
Homafar, A., Nasiri, H., Chelgani, S.C., 2022. Modeling Coking Coal Indexes by SHAP-XGBoost: Explainable Artificial Intelligence Method. Fuel Communications 13, 100078. https://doi.org/10.1016/j.jfueco.2022.100078.
Huang, L., Wei, S., Gao, C., Liu, N., 2022. Cyclical Adversarial Attack Pierces Black-Box Deep Neural Networks. Elsevier, Pattern Recognition, p. 108831.
Huo, W., Li, W., Zhang, Z., Sun, C., Zhou, F., Gong, G., 2021. Performance Prediction of Proton-Exchange Membrane Fuel Cell Based on Convolutional Neural Network and Random Forest Feature Selection. Energ. Conver. Manage. 243. Elsevier: 114367.
Hussain, Saddam, Mohd Wazir Mustafa, Touqeer A Jumani, Shadi Khan Baloch, Hammad Alotaibi, Ilyas Khan, and Afrasyab Khan. 2021. "A Novel Feature Engineered-CatBoost-Based Supervised Machine Learning Framework for Electricity Theft Detection." *Energy Reports* 7. Elsevier: 4425–4436.
Ibrahim, Abdullahi A, Raheem L Ridwan, Muhammed M Muhammed, Rabiat O Abdulaziz, and Ganiyu A Saheed. 2020. "Comparison of the CatBoost Classifier with Other Machine Learning Methods." *International Journal of Advanced Computer Science and Applications* 11 (11). Science and Information (SAI) Organization Limited.
Jabeur, S.B., Ballouk, H., Mefteh-Wali, S., Omri, A., 2022. Forecasting the Macrolevel Determinants of Entrepreneurial Opportunities Using Artificial Intelligence Models. Technol. Forecast. Soc. Chang. 175. Elsevier: 121353.
Je, J., Lee, D., Kwon, J., Cho, H., 2022. Simulation of Bubble-Particle Attachment Process and Estimation of Attachment Probability Using a Coupled Smoothed Particle Hydrodynamics-Discrete Element Method Model. Miner. Eng. 183. Elsevier: 107581.
Jones, E.J., Bishop, T.F.A., Malone, B.P., Hulme, P.J., Whelan, B.M., Filippi, P., 2022. Identifying Causes of Crop Yield Variability with Interpretive Machine Learning. Comput. Electron. Agric. 192. Elsevier: 106632.
Jorjani, E., Bagherieh, A.H., Mesroghli, Sh., Chehreh Chelgani, S., 2008. Prediction of Yttrium, Lanthanum, Cerium, and Neodymium Leaching Recovery from Apatite Concentrate Using Artificial Neural Networks. J. Univ. Sci. Technol. Beijing, Mineral, Metallurgy, Material 15 (4), 367–374.
Kang, P., Li, J., Jiang, S., Shull, P.B., 2022. Reduce System Redundancy and Optimize Sensor Disposition for EMG-IMU Multi-Modal Fusion Human-Machine Interfaces with XAI. IEEE, IEEE Transactions on Instrumentation and Measurement.
Kardani, N., Zhou, A., Nazem, M., Shen, S.-L., 2021. Improved Prediction of Slope Stability Using a Hybrid Stacking Ensemble Method Based on Finite Element Analysis and Field Data. J. Rock Mech. Geotech. Eng. 13 (1). Elsevier: 188–201.
Kellner, R., Nagl, M., Rösch, D., 2022. Opening the Black Box-Quantile Neural Networks for Loss given Default Prediction. J. Bank. Financ. 134. Elsevier: 106334.
LeCun, Y., Bottou, L., Bengio, Y., Haffner, P., 1998. Gradient-Based Learning Applied to Document Recognition. Proc. IEEE 86 (11). IEEE: 2278–2324.
Li, Y., Zhu, H., Li, W., Zhu, Y., 2019. A Fundamental Study of Chalcopyrite Flotation in Sea Water Using Sodium Silicate. Miner. Eng. 139. Elsevier: 105862.
Liang, Minfei, Ze Chang, Zhi Wan, Yidong Gan, Erik Schlangen, and Branko Šavija. 2022. "Interpretable Ensemble-Machine-Learning Models for Predicting Creep Behavior of Concrete." Cement and Concrete Composites 125. Elsevier: 104295.
Luo, Mi, Yifu Wang, Yunhong Xie, Lai Zhou, Jingjing Qiao, Siyu Qiu, and Yujun Sun. 2021. "Combination of Feature Selection and Catboost for Prediction: The First Application to the Estimation of Aboveground Biomass." Forests 12 (2). MDPI: 216.
Machado, Linnéa, and David Holmer. 2022. "Credit Risk Modelling and Prediction: Logistic Regression versus Machine Learning Boosting Algorithms.".
Maree, Westhein, Lourens Kloppers, Gregory Hangone, and Oluwaseun Oyekola. 2017. "The Effects of Mixtures of Potassium Amyl Xanthate (PAX) and Isopropyl Ethyl Thionocarbamate (IPETC) Collectors on Grade and Recovery in the Froth Flotation of a Nickel Sulfide Ore." South African Journal of Chemical Engineering 24 (1). South African Institution of Chemical Engineers (SAIChE): 116–121.
Mokgethwa, Meso Florence, Abraham Adewale Adeleke, Peter Mendonidis, and Mosobalaje Oyebamiji Adeoye. 2016. "An Evaluation of Sodium Ethyl Xanthate for the Froth Flotation Upgrading of a Carbonatitic Copper Ore." Journal of Physical Science 27 (2). Universiti Sains Malaysia Press: 13.
Muanda, M.M., Omalanga, P.P.D., Mitonga, V.M., 2021. Comparative Cleaning Stages in Recovery of Copper and Cobalt from Tailings Using Potassium Amylxanthate as Collector. Eur. J. Eng. Technol. Res. 6 (2), 96–100.
Nasiri, H., Ebadzadeh, M.M., 2022. MFRFNN: Multi-Functional Recurrent Fuzzy Neural Network for Chaotic Time Series Prediction. Neurocomputing 507. Elsevier, 292–310. https://doi.org/10.1016/j.neucom.2022.08.032.
Nasiri, H., Hasani, S., 2022. Automated Detection of COVID-19 Cases from Chest X-Ray Images Using Deep Neural Network and XGBoost. Radiography 28 (3), 732–738. https://doi.org/10.1016/j.radi.2022.03.011.
Nasiri, H., Homafar, A., Chelgani, S.C., 2021. Prediction of Uniaxial Compressive Strength and Modulus of Elasticity for Travertine Samples Using an Explainable Artificial Intelligence. Results Geophys. Sci. 8, 100034 https://doi.org/10.1016/j.ringps.2021.100034.
Nazari, S., Chehreh Chelgani, S., Shafaei, S.Z., Shahbazi, B., Matin, S.S., Gharabaghi, M., 2019. Flotation of Coarse Particles by Hydrodynamic Cavitation Generated in the Presence of Conventional Reagents. Sep. Purif. Technol. 220. Elsevier: 61–68.
Neethling, S.J., Cilliers, J.J., 2012. Grade-Recovery Curves: A New Approach for Analysis of and Predicting from Plant Data. Miner. Eng. 36. Elsevier: 105–110.
Ngobeni, W.A., Hangone, G., Ikhu-Omoregbe, D., 2013. The Froth Flotation of a Nickel Sulphide Ore Using Thiol Collectors and Their Mixtures. M. Tech Thesis. Department of Chemical Engineering. Cape Peninsula University of Technology, Bellville.
Palimkar, P., Shaw, R.N., Ghosh, A., 2022. Machine Learning Technique to Prognosis Diabetes Disease: Random Forest Classifier Approach. In: Advanced Computing and Intelligent Technologies. Springer, pp. 219–244.
Pan, Y., Bournival, G., Ata, S., 2021. The Role of Non-Frothing Reagents on Bubble Size and Bubble Stability. Miner. Eng. 161. Elsevier: 106652.
Pan, Y., Bournival, G., Ata, S., 2022a. Foaming Behaviour of Frothers in the Presence of PAX and Salt. Miner. Eng. 178. Elsevier: 107405.
Pan, Y., Gresham, I., Bournival, G., Prescott, S., Ata, S., 2022b. Synergistic Effects of Frothers, Collector and Salt on Bubble Stability. Powder Technol. 397. Elsevier: 117028.
Panahi, M., Sadhasivam, N., Pourghasemi, H.R., Rezaie, F., Lee, S., 2020. Spatial Prediction of Groundwater Potential Mapping Based on Convolutional Neural Network (CNN) and Support Vector Regression (SVR). J. Hydrol. 588. Elsevier: 125033.
Paryani, S., Neshat, A., Pourghasemi, H.R., Ntona, M.M., Kazakis, N., 2022. A Novel Hybrid of Support Vector Regression and Metaheuristic Algorithms for Groundwater Spring Potential Mapping. Sci. Total Environ. 807. Elsevier: 151055.
Pu, Y., Szmigiel, A., Chen, J., Apel, D.B., 2020. FlotationNet: A Hierarchical Deep Learning Network for Froth Flotation Recovery Prediction. Powder Technol. 375. Elsevier: 317–326.
Qiu, Y., Zhou, J., Khandelwal, M., Yang, H., Yang, P., Li, C., 2021. Performance Evaluation of Hybrid WOA-XGBoost, GWO-XGBoost and BO-XGBoost Models to Predict Blast-Induced Ground Vibration. Eng. Comput.. Springer 1–18.
Rabatho, Jan Pana, William Tongamp, Junji Kato, Kazutoshi HAGA, Yasushi TAKASAKI, and Atsushi SHIBAYAMA. 2011. "Effect of Flotation Reagents for Upgrading and Recovery of Cu and Mo from Mine Tailing by Flotation." Resources Processing 58 (1). The Resources Processing Society of Japan: 14–21.
Ramirez, A., Rojas, A., Gutierrez, L., Laskowski, J.S., 2018. Sodium Hexametaphosphate and Sodium Silicate as Dispersants to Reduce the Negative Effect of Kaolinite on the Flotation of Chalcopyrite in Seawater. Miner. Eng. 125. Elsevier: 10–14.
Sarvamangala, D.R., Kulkarni, R.V., 2022. Convolutional Neural Networks in Medical Image Understanding: A Survey. Evol. Intel. 15 (1). Springer: 1–22.
Sasikumar, A., Vairavasundaram, S., Ketan Kotecha, V., Indragandhi, L.R., Selvachandran, G., Abraham, A., 2022. Blockchain-Based Trust Mechanism for Digital Twin Empowered Industrial Internet of Things. Elsevier, Future Generation Computer Systems.
Shahbazi, B., Rezai, B., Chehreh Chelgani, S., Javad Koleini, S.M., Noaparast, M., 2013. Estimation of Diameter and Surface Area Flux of Bubbles Based on Operational Gas Dispersion Parameters by Using Regression and ANFIS. Int. J. Min. Sci. Technol. 23 (3). Elsevier: 343–348.
Shahbazi, B., Chehreh Chelgani, S., Matin, S.S., 2017. Prediction of Froth Flotation Responses Based on Various Conditioning Parameters by Random Forest Method. Colloids Surf A Physicochem Eng Asp 529. Elsevier: 936–941.
Sharma, G., Joshi, A.M., 2022. SzHNN: A Novel and Scalable Deep Convolution Hybrid Neural Network Framework for Schizophrenia Detection Using Multichannel EEG. IEEE Trans. Instrum. Meas. 71. IEEE: 1–9.
Tapley, B., Yan, D., 2003. The Selective Flotation of Arsenopyrite from Pyrite. Miner. Eng. 16 (11). Elsevier: 1217–1220.
Tikka, Jesse. 2014. "On-Line Determination of Residual Collector Concentration in Flotation Process." LAPPEENRANNAN TEKNILLINEN YLIOPISTO.
Tohry, A., Chehreh Chelgani, S., Matin, S.S., Noormohammadi, M., 2020. Power-Draw Prediction by Random Forest Based on Operating Parameters for an Industrial Ball Mill. Adv. Powder Technol. 31 (3). Elsevier: 967–972.
Tohry, A., Yazdani, S., Hadavandi, E., Mahmudzadeh, E., Chehreh Chelgani, S., 2021. Advanced Modeling of HPGR Power Consumption Based on Operational Parameters by BNN: A 'Conscious-Lab' Development. Powder Technol. 381. Elsevier: 280–284.
van der Velden, B.H.M., Kuijf, H.J., Gilhuijs, K.G.A., Viergever, M.A., 2022. Explainable Artificial Intelligence (XAI) in Deep Learning-Based Medical Image Analysis. Elsevier, Medical Image Analysis, p. 102470.
Vaulet, Thibaut, Maya Al-Memar, Hanine Fourie, Shabnam Bobdiwala, Srdjan Saso, Maria Pipi, Catriona Stalder, et al. 2022. "Gradient Boosted Trees with Individual Explanations: An Alternative to Logistic Regression for Viability Prediction in the First Trimester of Pregnancy." *Computer Methods and Programs in Biomedicine* 213. Elsevier: 106520.
Wang, H., Zhao, Y., Ji, H., Yuan, Zhenyu, Kong, Lu, Meng, Fanli, 2022. EEMD and GUCNN-XGBoost Joint Recognition Algorithm for Detection of Precursor Chemicals Based on Semiconductor Gas Sensor. IEEE Trans. Instrum. Meas. 71. IEEE: 1–12.
Wen, Zhiping, Changkui Zhou, Jinhe Pan, Tiancheng Nie, Changchun Zhou, and Zhaolin Lu. 2021. "Deep Learning-Based Ash Content Prediction of Coal Flotation Concentrate Using Convolutional Neural Network." Minerals Engineering 174. Elsevier: 107251.

Wen, X., Xie, Y., Lingtao, Wu., Jiang, L., 2021a. Quantifying and Comparing the Effects of Key Risk Factors on Various Types of Roadway Segment Crashes with LightGBM and SHAP. Accid. Anal. Prev. 159. Elsevier: 106261.

Wills, B.A., Finch, J., 2015. Wills' Mineral Processing Technology: An Introduction to the Practical Aspects of Ore Treatment and Mineral Recovery. Butterworth-Heinemann.

Wood, C.J., 1972. Some Factors Influencing the Rate of Flotation of Fine Galena Particles. University of New South Wales.

Xu, Wenjun, Jia Cui, Lan Li, Bitao Yao, Sisi Tian, and Zude Zhou. 2021. "Digital Twin-Based Industrial Cloud Robotics: Framework, Control Approach and Implementation." Journal of Manufacturing Systems 58. Elsevier: 196–209.

Zanin, M., Lambert, H., Du Plessis, C.A., 2019. Lime Use and Functionality in Sulphide Mineral Flotation: A Review. Miner. Eng. 143. Elsevier: 105922.

Zarie, M., Jahedsaravani, A., Massinaei, M., 2020. Flotation Froth Image Classification Using Convolutional Neural Networks. Miner. Eng. 155. Elsevier: 106443.

Zeng, H., Shao, B., Dai, H., Yan, Y., Tian, N., 2023. Prediction of Fluctuation Loads Based on GARCH Family-CatBoost-CNNLSTM. Energy 263. Elsevier: 126125.

Zhang, C.A., Cho, S., Vasarhelyi, M., 2022. Explainable Artificial Intelligence (XAI) in Auditing. Int. J. Account. Inf. Syst. 46. Elsevier: 100572.

Zhang, W., Chongzhi, Wu., Zhong, H., Li, Y., Wang, L., 2021. Prediction of Undrained Shear Strength Using Extreme Gradient Boosting and Random Forest Based on Bayesian Optimization. Geosci. Front. 12 (1). Elsevier: 469–477.

Zhang, Ning-Ning, Chang-Chun Zhou, Jin-He Pan, Wencheng Xia, Cheng Liu, Meng-Cheng Tang, and Shan-Shan Cao. 2017. "The Response of Diasporic-Bauxite Flotation to Particle Size Based on Flotation Kinetic Study and Neural Network Simulation." Powder Technology 318. Elsevier: 272–281.

Zhang, Y., Zhu, J., Liu, T., 2012. The Research of the Flotation Recovery Prediction Methods Based on Advanced LS-SVM. Appl. Mech. Mater. 130, 1854–1857.

Zhou, Kaibo, Shangyuan Li, Xiang Zhou, Yangxiang Hu, Changhe Zhang, and Jie Liu. 2021. "Data-Driven Prediction and Analysis Method for Nanoparticle Transport Behavior in Porous Media." Measurement 172. Elsevier: 108869.